Please cite this article in press as: Dondelinger et al., MLKL Compromises Plasma Membrane Integrity by Binding to Phosphatidylinositol Phosphates, Cell Reports (2014), http://dx.doi.org/10.1016/j.celrep.2014.04.026

Cell Reports
Report

MLKL Compromises Plasma Membrane Integrity by Binding to Phosphatidylinositol Phosphates

Yves Dondelinger,[1,2] Wim Declercq,[1,2] Sylvie Montessuit,[3] Ria Roelandt,[1,2] Amanda Goncalves,[4] Inge Bruggeman,[1,2] Paco Hulpiau,[1,2] Kathrin Weber,[1,2] Clark A. Sehon,[5] Robert W. Marquis,[5] John Bertin,[5] Peter J. Gough,[5] Savvas Savvides,[6] Jean-Claude Martinou,[3] Mathieu J.M. Bertrand,[1,2] and Peter Vandenabeele[1,2,7,*]

[1]VIB Inflammation Research Center, Technologiepark 927, 9052 Zwijnaarde-Ghent, Belgium
[2]Department of Biomedical Molecular Biology, Ghent University, Technologiepark 927, 9052 Zwijnaarde-Ghent, Belgium
[3]Department of Cell Biology, University of Geneva, 1211 Geneva 4, Switzerland
[4]Microscopy Core Facility, VIB Inflammation Research Center, VIB/Ghent University, Technologiepark 927, 9052 Zwijnaarde-Ghent, Belgium
[5]Pattern Recognition Receptor Discovery Performance Unit, Immuno-Inflammation Therapeutic Area, GlaxoSmithKline, Collegeville, PA 19426, USA
[6]Unit for Structural Biology and Biophysics, Laboratory for Protein Biochemistry and Biomolecular Engineering, Ghent University, K.L. Ledeganckstraat 35, 9000 Ghent, Belgium
[7]Methusalem Program, Ghent University, Technologiepark 927, 9052 Zwijnaarde-Ghent, Belgium
*Correspondence: peter.vandenabeele@irc.vib-ugent.be
http://dx.doi.org/10.1016/j.celrep.2014.04.026

SUMMARY

Although mixed lineage kinase domain-like (MLKL) protein has emerged as a specific and crucial protein for necroptosis induction, how MLKL transduces the death signal remains poorly understood. Here, we demonstrate that the full four-helical bundle domain (4HBD) in the N-terminal region of MLKL is required and sufficient to induce its oligomerization and trigger cell death. Moreover, we found that a patch of positively charged amino acids on the surface of the 4HBD binds to phosphatidylinositol phosphates (PIPs) and allows recruitment of MLKL to the plasma membrane. Importantly, we found that recombinant MLKL, but not a mutant lacking these positive charges, induces leakage of PIP-containing liposomes as potently as BAX, supporting a model in which MLKL induces necroptosis by directly permeabilizing the plasma membrane. Accordingly, we found that inhibiting the formation of PI(5)P and PI(4,5)P_2 specifically inhibits tumor necrosis factor (TNF)-mediated necroptosis but not apoptosis.

INTRODUCTION

Necroptosis is a caspase-independent form of cell death that contributes to the pathogenesis of several human diseases, including ischemia-reperfusion injury, sepsis, and viral infection (Duprez et al., 2011; Linkermann et al., 2013; Mocarski et al., 2012). Understanding the molecular mechanisms regulating necroptosis is therefore an important priority that may lead to the development of new therapies for the treatment of these diseases. Signal transduction during necroptosis has so far been mostly studied in the context of tumor necrosis factor (TNF). In most cells, TNF receptor 1 engagement promotes cell survival by assembly of a plasma membrane-associated complex, known as complex I, which activates the canonical nuclear factor κ B cell (NF-κB) pathway and drives expression of prosurvival molecules. Inhibition of the NF-κB response consequently switches the prosurvival signal to a caspase-8-dependent apoptotic trigger (Vanden Berghe et al., 2014). Under specific conditions, such as cIAP1/cIAP2 depletion or transforming growth factor β-activated kinase-1 (TAK1) kinase inhibition, apoptosis induction was shown to rely on receptor-interacting serine/threonine-protein kinase 1 (RIPK1) kinase activity (Biton and Ashkenazi, 2011; Dondelinger et al., 2013; Wang et al., 2008). When caspase-8 activation is compromised, apoptosis is inhibited, and the enzymatic activity of RIPK1 alternatively regulates the formation of the necrosome, a necroptosis-inducing complex consisting of RIPK1, RIPK3 (Cho et al., 2009; He et al., 2009; Zhang et al., 2009), and mixed lineage kinase domain-like (MLKL) protein (Sun et al., 2012; Zhao et al., 2012). Within this complex, RIPK1 and RIPK3 bind to each other by homotypic RIP homotypic interaction motif-domain interactions, allowing them to form amyloid-like fibrillar structures (Li et al., 2012). MLKL is recruited to the necrosome via interaction of its kinase-like domain (KLD) with the kinase domain of RIPK3 (Sun et al., 2012; Xie et al., 2013), which subsequently leads to MLKL activation by RIPK3-mediated phosphorylation (Sun et al., 2012; Murphy et al., 2013).

Activated MLKL was suggested to further transduce the necroptotic signal by binding and activating phosphoglycerate mutase 5 (PGAM5), a signal for dynamin-related protein 1 (DRP1)-mediated mitochondrial fragmentation and subsequent necroptosis induction (Wang et al., 2012). However, recent studies have challenged the importance of PGAM5 and DRP1 in necroptosis induction (Murphy et al., 2013; Remijsen et al., 2014; Tait et al., 2013). In line with this, mitochondria-depleted cells were shown to maintain their ability to die by necroptosis (Tait et al., 2013), therefore questioning the importance of the mitochondrial axis in the induction of this cell death modality.

Please cite this article in press as: Dondelinger et al., MLKL Compromises Plasma Membrane Integrity by Binding to Phosphatidylinositol Phosphates, Cell Reports (2014), http://dx.doi.org/10.1016/j.celrep.2014.04.026

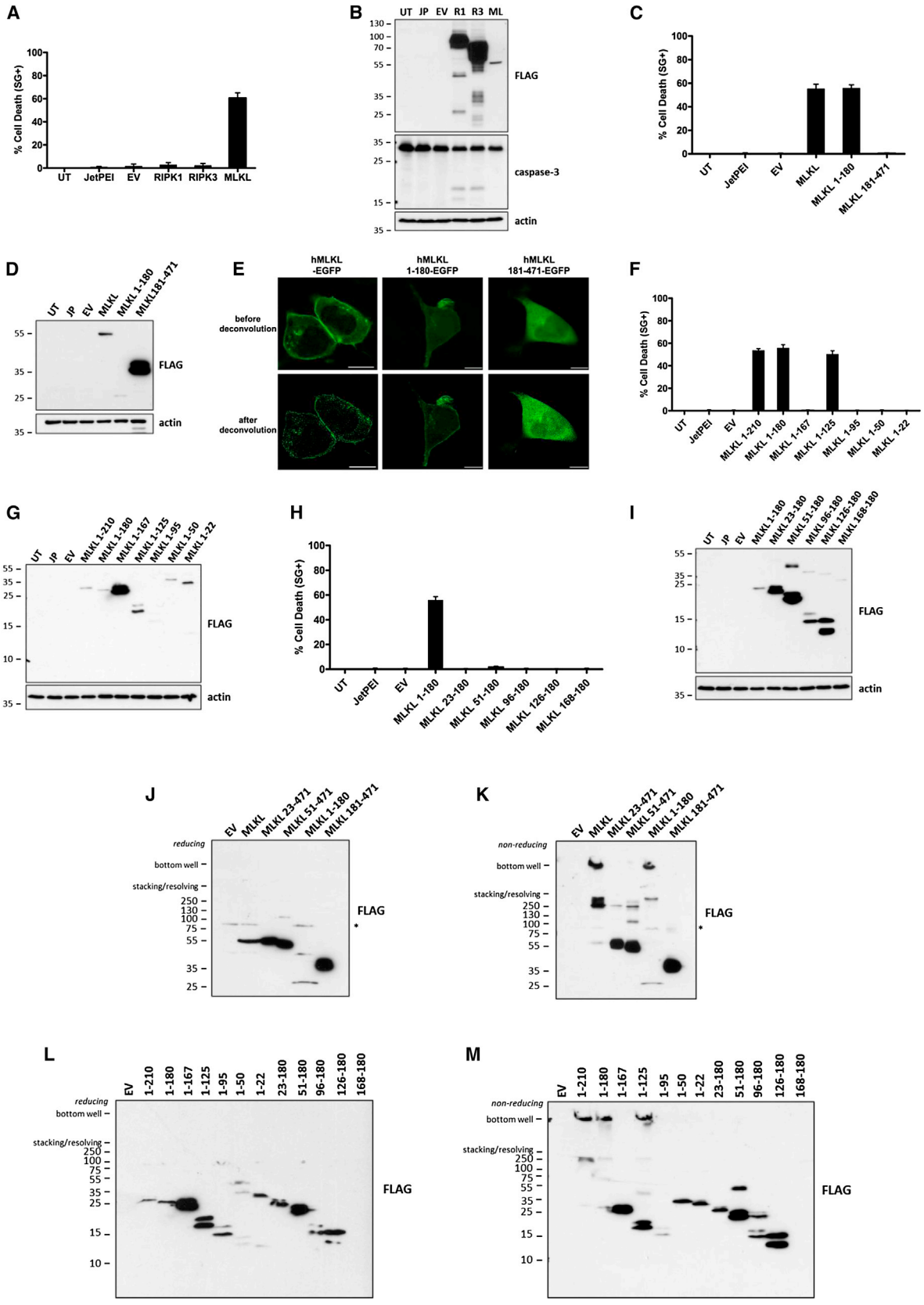

(legend on next page)

In this study, we demonstrate that MLKL translocates to the plasma membrane upon induction of necroptosis, where it interacts with phosphatidylinositol phosphates (PIPs) via a patch of positively charged amino acids at the surface of a four-helical bundle domain (4HBD) located in its N-terminal region. Importantly, we found that this domain is sufficient to induce leakage of PIP-containing liposomes. From these findings, a model can be inferred: MLKL mediates cell death by permeabilizing PIP-containing membranes.

RESULTS

The Full 4HBD of MLKL Is Required and Sufficient for Necroptosis Induction

Contrary to RIPK1 and RIPK3, MLKL has been reported to specifically transduce TNF-mediated necroptosis, and not apoptosis (Biton and Ashkenazi, 2011; Dondelinger et al., 2013; Murphy et al., 2013; Wang et al., 2008; Wu et al., 2013). In addition, MLKL was shown to act downstream of RIPK1/RIPK3 during necroptosis induction (Chen et al., 2014; Murphy et al., 2013; Sun et al., 2012). In order to specifically study the molecular events occurring at the level or downstream of MLKL during necroptosis, we decided to ectopically express MLKL in human embryonic kidney 293T (HEK293T) cells. As previously reported by Zhao et al. (2012), MLKL expression was highly toxic and, contrary to RIPK1 or RIPK3, not associated with caspase-3 activation (Figures 1A and 1B). MLKL-induced cell death was characterized by hallmarks of necroptosis, such as cell swelling and the appearance of a translucent cytoplasm before plasma membrane rupture and propidium iodide positivity (Figure S1A). Accordingly, the pan-caspase inhibitor zVAD-fmk did not protect cells from death induced by MLKL overexpression (Figure S1B). To investigate the role of endogenous RIPK1 and RIPK3 in our system, we tested the effect of inhibiting their kinase activities by using the RIPK1 kinase inhibitor necrostatin-1 (Nec-1) and the RIPK3 inhibitor (R3i) GSK'840 (Figure S4). Neither Nec-1 nor R3i protected the cells from MLKL-induced necroptosis, whereas they potently inhibited TNF/TAK1i/zVAD-fmk-induced necroptosis in HT-29 cells (Figures S1C and S1D). Together, these results confirmed the establishment of a model system to specifically study the molecular events occurring at the level or downstream of MLKL during necroptosis.

MLKL consists of an N-terminal 4HBD fused by a brace region (BR) to a C-terminal inactive KLD (Murphy et al., 2013). To identify the region of MLKL that mediates cytotoxicity in our system, we individually expressed the 4HBD–BR (amino acids 1–180) and KLD (amino acids 181–471) and found that the 4HBD–BR was sufficient to induce necroptosis (Figures 1C and 1D). We fused full-length MLKL, N-terminal 4HBD–BR, and C-terminal KLD to GFP and analyzed the subcellular localization of the different fusion proteins by confocal microscopy. We observed that both full-length MLKL and the 4HBD–BR mutant were recruited to the plasma membrane, whereas the KLD mutant remained cytoplasmic (Figure 1E), indicating that recruitment to the plasma membrane correlates with the killing potential of MLKL.

In silico analysis combined with homology studies based on the recently solved crystal structure of mouse MLKL (Murphy et al., 2013) allowed us to predict the structure of human MLKL and to delineate the four α helixes contained within its N-terminal 4HBD (amino acids 1–125) and the two in its BRs (amino acids 125–181) (Figure S1E). To investigate the contribution of the different α helixes in necroptotic cell death, we generated C-terminal (Figures 1F and 1G) and N-terminal (Figures 1H and 1I) deletion fragments of the 4HBD–BR and found that the four α helixes of 4HBD (1–125) were required and sufficient to induce necroptotic cell death (Figure 1F). Intriguingly, a truncation mutant with a partial BR (1–167) was unable to induce necroptosis, suggesting that the complete BR stabilizes the killing potential of MLKL. Of note, we found that only the necroptosis-inducing constructs (full-length MLKL, 4HBD–BR, 1–210 MLKL, 1–180 MLKL, and 1–125 MLKL) formed high molecular weight (HMW) oligomers upon expression, as observed by enormous upshifts in nonreducing SDS-PAGE (Figures 1J–1M and S1F). These results indicated a clear correlation between formation of HMW oligomers on nonreducing PAGE and necroptosis induction.

Positive Charges in the Four-Helical Bundle of MLKL Are Required for Recruitment of MLKL to the Plasma Membrane, Its Oligomerization, and the Induction of Necroptosis

Given the correlation between necroptosis induction and plasma membrane recruitment, we investigated whether MLKL directly binds to plasma membrane components to mediate its cytotoxicity. Protein-membrane interactions can be mediated by a broad spectrum of protein domains, including C1, C2, PH, FYVE, PX, ENTH, ANTH, BAR, and FERM domains (Cho and Stahelin, 2005). A universal theme is that protein-membrane interaction is regulated by electrostatic interactions between the negatively charged phospholipids of the plasma membrane and the positively charged amino acids in a domain of the membrane-binding protein. Because the 4HBD is sufficient to induce necroptosis after ectopic expression, we investigated whether it

Figure 1. The Full 4HBD of MLKL Is Required and Sufficient for Necroptosis Induction

HEK293T cells were left untreated, treated with the jetPEI transfection reagent alone, or transfected with 1 μg of an empty vector or with pLenti6-strep-CDS-FLAG vectors encoding the indicated proteins. After 24 hr, cell death was quantified by SYTOX Green staining (A, C, F, and H), and protein expression levels were analyzed by immunoblotting (B, D, G, and I). Cell death data are presented as mean ± SEM of three independent experiments. R1, pLenti6-strep-hRIPK1-FLAG; R3, pLenti6-strep-hRIPK3-FLAG; ML, pLenti6-strep-hMLKL-FLAG.

(E) HEK293T cells were transfected with 50 ng of the indicated pLenti6-strep-hMLKL-EGFP mutants, and GFP fluorescence was analyzed the next day by confocal microscopy. Scale bars, 15 μM.

(J–M) HEK293T cells were transfected with 1 μg of empty vector or the indicated pLenti6-strep-hMLKL-FLAG mutants. After 24 hr, cells were lysed in 1× Laemmli buffer with 50 mM dithiothreitol (DTT) (reducing) or without (nonreducing). Cell lysates were analyzed by immunoblotting as indicated.

See also Figure S1.

Please cite this article in press as: Dondelinger et al., MLKL Compromises Plasma Membrane Integrity by Binding to Phosphatidylinositol Phosphates, Cell Reports (2014), http://dx.doi.org/10.1016/j.celrep.2014.04.026

contains a patch rich in positively charged amino acids. Interestingly, the region between amino acids 22 and 35 contains nine positively charged amino acids, and some of those are evolutionarily conserved between species (Figure 2A). To test whether these residues are involved in plasma membrane recruitment, we mutated all of them to the neutral amino acid alanine (9posA) or to the negatively charged glutamate residue (9posE). The side chains of these positively charged amino acids are solvent accessible at the surface of MLKL and do not contribute to intramolecular interactions. Therefore, we assumed that inverting the charge of these amino acids would not interfere with the overall protein structure. Additionally, a secondary structure prediction analysis revealed that these mutations would not alter the secondary structure of MLKL (data not shown). When ectopically expressed in cells, these mutants could no longer induce necroptosis, though they were expressed at much higher levels than the wild-type lethal counterparts (Figures 2B, 2C, and S2A). Using GFP-fusion constructs, we observed that these two mutants were not recruited to the plasma membrane anymore but instead were mainly found in the cytoplasm (Figures 2D and S2B).

Interestingly, we found that both the MLKL 9posA and 9posE mutants did not oligomerize anymore, suggesting that recruitment to the plasma membrane is necessary for oligomerization of MLKL (Figures 2E and 2F). To further validate the need of plasma membrane recruitment for MLKL's cytotoxicity, we performed a competition experiment with a positively charged probe modeled on the C-terminal part of K-Ras fused to GFP (posKRas), which has been shown to be recruited to the plasma membrane by electrostatic interactions (Yeung et al., 2006). Remarkably, we observed that posKRas cotransfection inhibited MLKL-induced cell death (Figures 2F–2H). In summary, these results indicate that highly conserved positive charges within the first two α helixes of the 4HBD of MLKL are required for recruitment of MLKL to the plasma membrane, for MLKL oligomerization, and for induction of necroptosis.

MLKL Interacts with PIPs by Positive Charges in Its N-Terminal Four-Helical Bundle

The functions of plasma membrane-associated proteins are often regulated by interaction with specific phospholipids in the plasma membrane. Therefore, we investigated whether MLKL binds to specific phospholipids. We produced a recombinant glutathione S-transferase (GST)-fused N-terminal fragment of MLKL (4HBD–BR), cleaved off the GST tag, and incubated the protein on a lipid array. We found that the N-terminal MLKL directly interacted with PIPs, but not with nonphosphorylated PI or other phospholipids (Figure 3A, upper panel). We next incubated the recombinant N-terminal MLKL with a specific PIP lipid array and found that MLKL could bind to most PIP species in vitro (Figure 3A, lower panel), whereas the recombinant MLKL 9posE mutant was unable to bind to PIPs on these arrays, further demonstrating that the interaction between MLKL and PIPs is mediated by the positively charged patch identified on the surface of MLKL (Figure 3A). Pleckstrin homology (PH) domains are protein domains of about 120 amino acids known to bind to PIP-containing lipids. Interestingly, different PH domains have different specificities for distinct PIPs. For example, the PH domain of phospholipase C δ (PLCδ) mainly binds to phosphatidylinositol (4,5)-diphosphate (PI(4,5)P_2) (Figure S3A; PI(4,5)P_2 GRIP), whereas the PH domain of Bruton's tyrosine kinase (BTK) has a specificity toward phosphatidylinositol (3,4,5)-triphosphate (PI(3,4,5)P_3) (Garcia et al., 1995; Rameh et al., 1997; Salim et al., 1996). To investigate whether binding of MLKL to PIPs is required for the induction of cell death, we performed a competition experiment by cotransfecting increasing amounts of PH-PLCδ and PH-BTK. Remarkably, we found that expression of either PH domain protected against MLKL-induced necroptosis (Figures 3B–3E). Of note, their coexpression greatly increased their inhibitory potential. These results indicate that MLKL binds PIPs via the positive charges of its 4HBD and has a broader affinity for PIPs than the PH domains of BTK and PLCδ taken separately. Taken together, these results indicate that binding of MLKL to PIPs is crucial for necroptosis execution.

The Interaction between MLKL and PIPs Permeabilizes Liposomes

Our in silico analysis revealed that the 4HBD of MLKL has structural similarities with α-pore-forming toxins (data not shown). These bacterial toxins consist of helical bundle domains that can oligomerize into cytolytic pores in the plasma membrane (Parker and Feil, 2005). Because MLKL oligomerization and translocation to the plasma membrane are required for its killing potential, we investigated whether MLKL itself has pore-forming capacities. To do so, we incubated the recombinant N-terminal domain of MLKL (4HBD–BR), which is sufficient for necroptosis induction in cells (Figure 1F), with phosphatidycholine (PC) liposomes containing 5% PI, phosphatidylinositol (5)-phosphate (PI(5)P), PI(4,5)P_2, or PI(3,4,5)P_3. We observed that this MLKL easily released carboxyfluorescein (CF) from liposomes containing PI(5)P, PI(4,5)P_2, or PI(3,4,5)P_3, but not from PI-containing liposomes (Figures 4A–4D). When we compared the activity of N-terminal MLKL to the activity of the known pore-former BCL2-associated X protein (BAX), we found that this MLKL was as potent as BAX in permeabilizing liposomes (Figures 4A–4D). These results indicate that MLKL, and more precisely its 4HBD, has intrinsic capacities to permeabilize membranes. Interestingly, BAX was also able to induce lysis of PI-containing liposomes, whereas MLKL clearly was not, highlighting the clear dependency of MLKL for PIPs in permeabilizing liposomes. This is consistent with the results obtained with the lipid arrays, which showed that recombinant MLKL bound to PIP, PI(4,5)P_2, and PI(3,4,5)P_3, but not to PI. Importantly, the MLKL 9posE mutant was unable to permeabilize the PIP-containing liposomes (Figures 4A–4D), demonstrating the crucial role of the positive patch in the recruitment and function of MLKL at the membrane. Collectively, these results demonstrate that MLKL can potently and specifically rupture PIP-containing liposomes, and suggest that MLKL permeabilizes the plasma membrane by binding to PIPs.

Interfering with the Formation of PI(5)P or PI(4,5)P_2 Inhibits TNF-Induced Necroptosis but Not TNF-Induced Apoptosis

To validate our findings on the importance of the MLKL-PIP interaction for the execution of necroptosis in a physiological context,

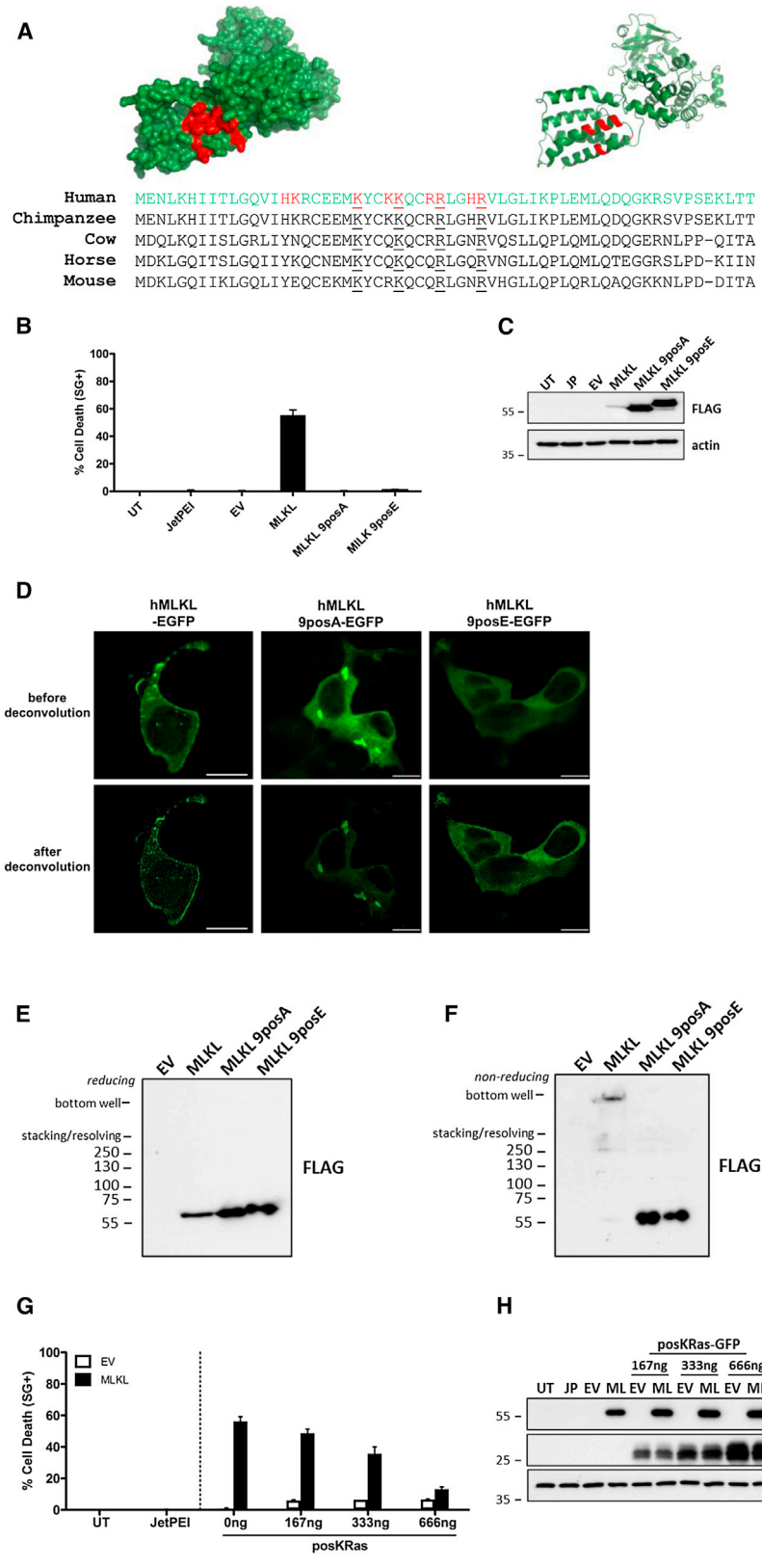

Figure 2. Positive Charges in the Four-Helical Bundle of MLKL Are Required for Recruitment of MLKL to the Plasma Membrane, Its Oligomerization, and the Induction of Necroptosis

(A) MLKL (green) contains a patch of positively charged amino acids (red) in the 4HBD. Some of the positively charged amino acids are conserved among species (underlined).

(B and C) HEK293T cells were transfected with 1 μg of empty vector or the indicated pLenti6-strep-hMLKL-FLAG mutants. After 24 hr, cell death was quantified by SYTOX Green staining (B), and protein expression levels were analyzed by immunoblotting (C).

(D) HEK293T cells were transfected with 50 ng of pLenti6-strep-hMLKL-EGFP mutants, and GFP fluorescence was analyzed the next day by confocal microscopy. Scale bars, 15 μM.

(E and F) HEK293T cells were transfected with 1 μg of empty vector or the indicated pLenti6-strep-hMLKL-FLAG mutants. After 24 hr, cells were lysed in 1× Laemmli buffer with 50 mM DTT (reducing) or without (nonreducing). Cell lysates were analyzed by immunoblotting, as indicated.

(G and H) HEK293T cells were transfected with 333 ng of empty vector or pLenti6-strep-hMLKL-FLAG in the presence of increasing concentrations of the posKRas plasmid. After 24 hr, cell death was quantified by SYTOX Green staining (G), and protein expression levels were analyzed by immunoblotting (H). Cell death data are presented as mean ± SEM of three independent experiments. See also Figure S2.

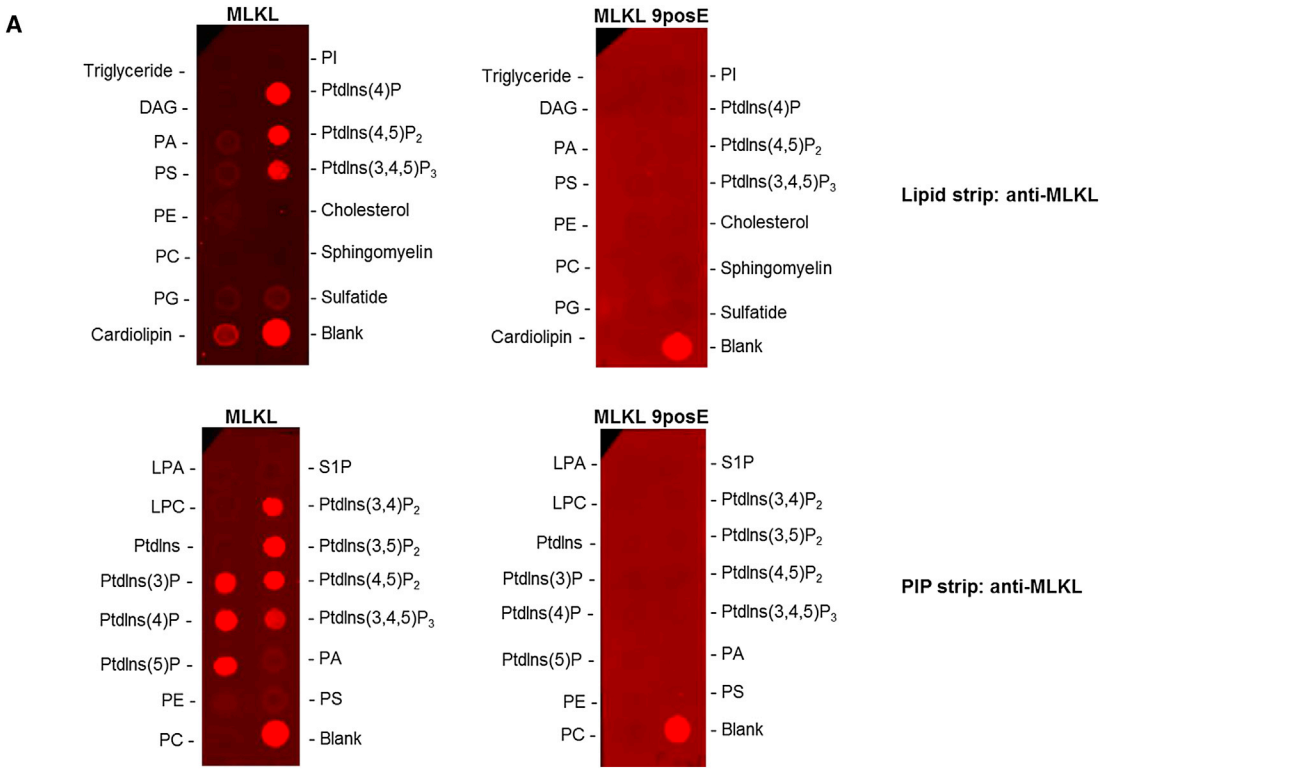

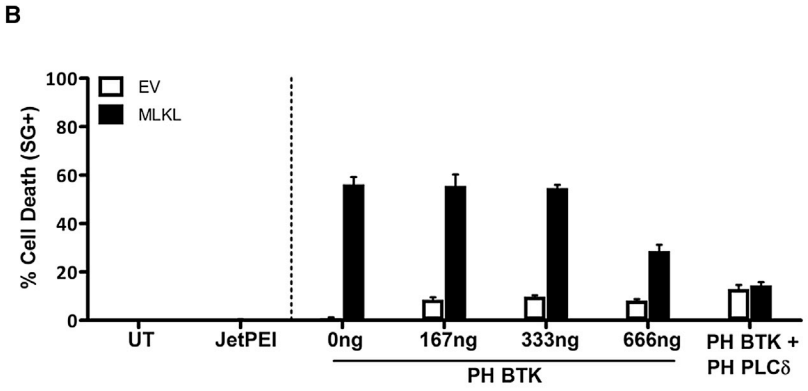

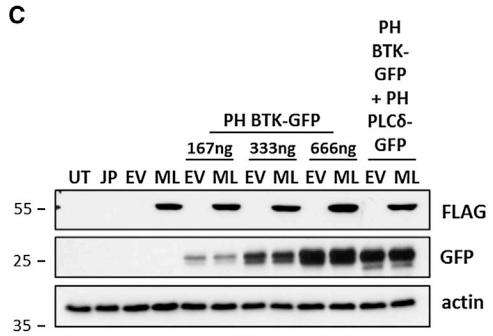

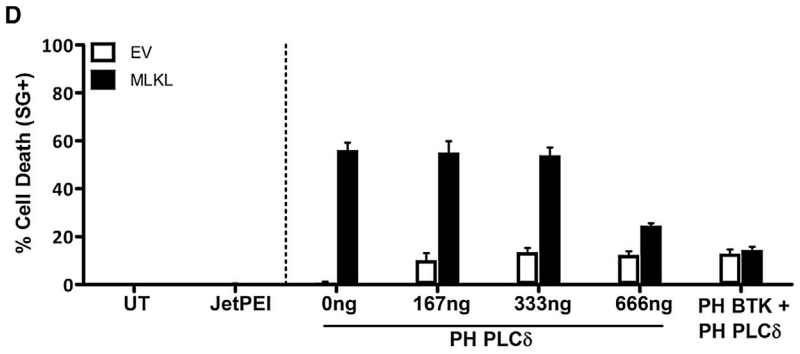

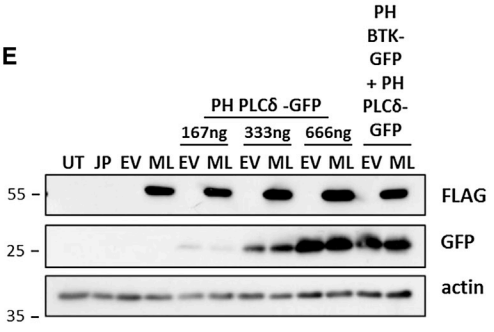

(legend on next page)

we tested the effect of several inhibitors of proteins involved in the formation of PIPs on TNF-induced necroptosis. We found that the inhibitor of PIKfyve (P5i), the enzyme responsible for the production of most intracellular PI(5)P, efficiently inhibited TNF-induced necroptosis in both the mouse L929sAhFas cell line (Figures 5A and 5B) and the human FADD$^{-/-}$ Jurkat cell line (Figures 5C and 5D). The inhibitor of phosphatase and tensin homolog (PTEN) (SF1670), which dephosphorylates PI(3,4,5)P_3 to PI(4,5)P_2, also reduced cell death induced by TNF, as did the PI(3,4,5)P_3 antagonist PITenin-7 (PIT-7). Interestingly, the combination of the PTEN and PIKfyve inhibitors blocked TNF-induced necroptosis even more potently in both cell lines (Figures 5A–5D). In contrast, the PI 3-kinase inhibitor 3MA did not affect TNF-induced necroptosis. We previously demonstrated that TNF-induced necroptosis in L929sA can be switched to a rapid induction of apoptosis by the knockdown of RIPK1 (Vanlangenakker et al., 2011). We generated a stable L929sAhFas cell line expressing either a nontargeting microRNA (miRNA) or a RIPK1 miRNA. When testing the PTEN and PIKfyve inhibitors separately or in combination on both transduced cell lines, we found that they inhibited TNF-induced necroptosis, but not TNF-induced apoptosis (Figures 5E and 5F). These results demonstrate a crucial and specific role of PIPs in TNF-mediated necroptosis, which supports our model of MLKL acting as a pore-forming molecule in PIP-containing membranes. The fact that simultaneous interference with the production of both PI(5)P and PI(4,5)P_2 efficiently and specifically inhibited TNF-induced necroptosis suggests that in these cell lines, MLKL is preferentially recruited to these PIPs.

DISCUSSION

It is becoming clear that necroptosis plays an important role in health and disease (Vanden Berghe et al., 2014; Vanlangenakker et al., 2008). Although necroptosis has a beneficial role in host defense against viral infections by clearing virus-infected cells and by activating the immune system through the release of damage-associated molecular patterns, it can also be detrimental and contribute to different pathologies when activated by death receptors in other contexts (Kaczmarek et al., 2013; Mocarski et al., 2012). Although our understanding of the upstream events leading to necrosome formation and RIPK3/MLKL activation has greatly increased lately, the downstream molecular mechanisms of necroptosis execution are still poorly understood. Several potential downstream events have been associated with necroptotic cell death, including integrity of mitochondria and lysosomes, Ca^{2+} signaling, and reactive oxygen species generation (Vanden Berghe et al., 2014). However, none of them was consistently associated with necroptosis in every cell type. This led to the hypothesis that several cell death subroutines might contribute to pulling the final trigger during necroptosis.

MLKL and the necrosome have been observed in various subcellular compartments, such as the cytosol (Sun et al., 2012), mitochondrial fraction (Wang et al., 2012), mitochondrial-associated membrane fraction (Chen et al., 2013), and very recently also the plasma membrane (Cai et al., 2014; Chen et al., 2014; Wang et al., 2014). In line with the latter reports, we observed plasma membrane localization, and our study additionally provides a molecular mechanism explaining the recruitment of MLKL to the plasma membrane. Indeed, we identified a positively charged patch in the 4HBD of MLKL that is required for PIPs binding and plasma membrane recruitment. We also report that plasma membrane localization is associated with the ability of MLKL to kill, and demonstrate that interfering with plasma membrane recruitment or PIP binding, respectively, by competitive assays using KRas or PH domain expression, blocked MLKL cytotoxicity.

Our in vitro liposome experiments revealed that MLKL specifically induces leakage of PIP-containing liposomes, raising the possibility that upon binding to PIPs at the plasma membrane, MLKL assembles into a pore that would facilitate the osmosis-mediated rupture of the membrane. Remarkably, we demonstrate that inhibiting formation of certain PIP species protects human and mouse cells from TNF-mediated necroptosis, but not apoptosis, a cell death modality that does not affect the plasma membrane integrity. Using nonreducing SDS-PAGE, we demonstrate that only the necroptosis-inducing constructs were associated with the occurrence of HMW forms of MLKL, whereas all other noncytotoxic MLKL deletion mutants displayed mobility at the predicted molecular weights. The observation of HMW forms of MLKL does not exclude the existence of the previously described trimers, tetramers, or hexamers (Cai et al., 2014; Chen et al., 2014; Wang et al., 2014), which may represent an earlier phase in the HMW complex formation process. It is indeed conceivable that MLKL pore formation works similarly to the BH3-in groove Bcl-2 antagonist/killer and BAX homodimers, which upon activation, expose a hydrophobic surface that initiates HMW pore-forming structures (Czabotar et al., 2014). Moreover, the formation of these HMW complexes is only observed when the full PIP-binding 4HBD is present. At this stage, we can only speculate on the pore size and on whether this is an ion-permeable or water-permeable pore, or even an active channel. Interestingly, two recent publications have functionally connected MLKL to two different ion channel mechanisms. In the first study, the authors report a role of MLKL in regulating extracellular calcium influx from the transient receptor potential melastatin-related 7 (Cai et al., 2014). In the

Figure 3. MLKL Interacts with PIPs by Positive Charges in Its N-Terminal Four-Helical Bundle

(A) Recombinant GST-hMLKL 1–210 or GST-hMLKL 1–210 9posE was incubated with PreScission protease to remove the GST tag and then incubated individually with a general lipid strip (upper panel) or a PIP strip (lower panel). Binding was revealed by immunoblotting with anti-MLKL with the Odyssey detection system. The "Blank" is spotted with xylene cyanol, and this interfered with detection in the red channel.

(B–E) HEK293T cells were transfected with 333 ng of the empty vector or the pLenti6-strep-hMLKL-FLAG plasmid in the presence of increasing concentrations of either PH-BTK or PH-PLCδ plasmid. Whenever combined, these latter plasmids were used at 333 ng each. After 24 hr, cell death was quantified by SYTOX Green staining (B and D), and protein expression levels were analyzed by immunoblotting (C and E). Cell death data are presented as mean ± SEM of three independent experiments.

See also Figure S3.

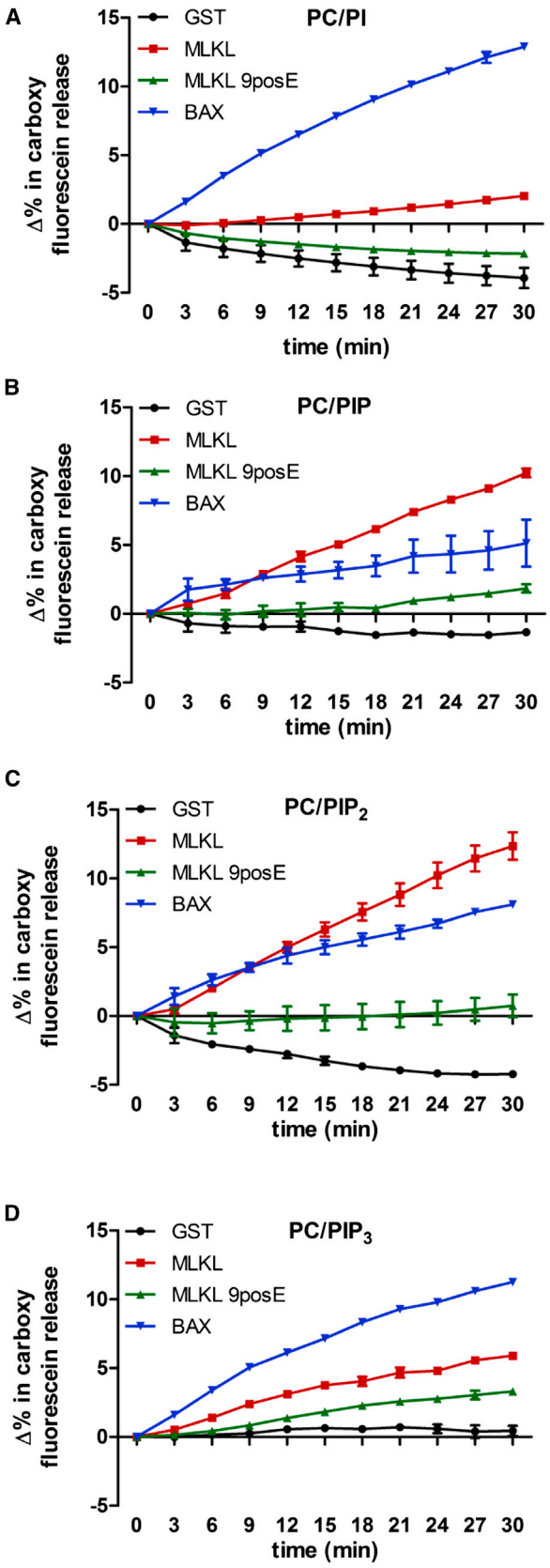

Figure 4. The Interaction between MLKL and PIPs Permeabilizes Liposomes

Liposomes consisting of 95% PC supplemented with (A) 5% PI(3,4,5)P_3, (B) 5% PI(4,5)P_2, (C) 5% PI(5)P, or (D) 5% PI were incubated with 500 nM of the indicated recombinant proteins of which GST was clipped. GST was included to control for any residual GST still present in the recombinant protein samples. CF release was measured in function of time using a CYT3F Cytation3 Cell Imaging Multi-Mode Microplate Reader. The data were normalized to put the percent CF release at 0% at time point 0 by subtracting the percent CF release at time point 0 for every measurement. The data are presented as mean ± SD of replicates of one representative experiment.

second one, MLKL function was associated with sodium influx (Chen et al., 2014). Our findings that MLKL binds PIPs and induces PIP-containing liposome leakage support a model in which the PIPs function to recruit MLKL to the membrane where it oligomerizes and forms a pore, therefore arguing for a direct pore-forming capacity of MLKL rather than for a role of MLKL in regulating other channels. However, a model combining our findings and those from these two recent publications can not be excluded. The PIPs that are associated with MLKL in the plasma membrane may facilitate the functioning of ion channels and transporters. Indeed, many ion channels and transporters require PI(4,5)P_2 for proper functioning (Suh and Hille, 2008). It is therefore conceivable that MLKL can act as a direct pore and that the associated PIPs may facilitate ion influx through channels and transporters, disturbing the osmotic homeostasis of the cell and leading to the typical cell swelling (“oncosis”) associated with necroptosis (Vanden Berghe et al., 2010). Very recently, another paper independently found that the recombinant N-terminal domain of MLKL is able to induce leakage of cardiolipin- or PIP-containing liposomes, suggesting a direct role of MLKL in membrane rupture (Wang et al., 2014). Importantly, a direct plasma membrane pore-forming capability of MLKL is consistent with data supporting the view that necroptosis induction is independent of the mitochondria (Murphy et al., 2013; Remijsen et al., 2014; Tait et al., 2013). Finally, our finding that the MLKL-PIP interaction is of crucial importance for necroptosis induction opens doors for the development of new compounds targeting the MLKL-PIP interaction, which will have great scientific and therapeutic benefits.

EXPERIMENTAL PROCEDURES

Plasmids

The sequences encoding wild-type RIPK1, RIPK3, and MLKL and the mutated and truncated versions of MLKL were cloned into pENTR3C using the CloneEZ PCR Cloning Kit (GenScript). The sequence encoding an N-terminal Strep-tag was fused directly to the coding sequence of all the used plasmids by PCR. Next, these sequences were transferred into homemade modified pLenti6 vectors, i.e., pLenti6-FLAG-puromycin or pLenti6-EFGP-V5-BLAST destination vector, using the LR Gateway recombination system (Life Technologies). The plasmid encoding a modified version of the positively charged C-terminal part of KRas (Addgene plasmid 17274) has been described elsewhere by Yeung et al. (2006). The plasmids containing the PH domains of BTK and PLCδ were a kind gift from J. Gettemans (Nanobody Lab, Department of Biochemistry, Ghent University).

Cell Lines

HEK293T and L929sAhFas cells were cultured in Dulbecco’s modified Eagle’s medium supplemented with 10% fetal calf serum (FCS), L-glutamine (200 mM), and sodium pyruvate (400 mM). HT-29 cells were cultured in Eagle’s

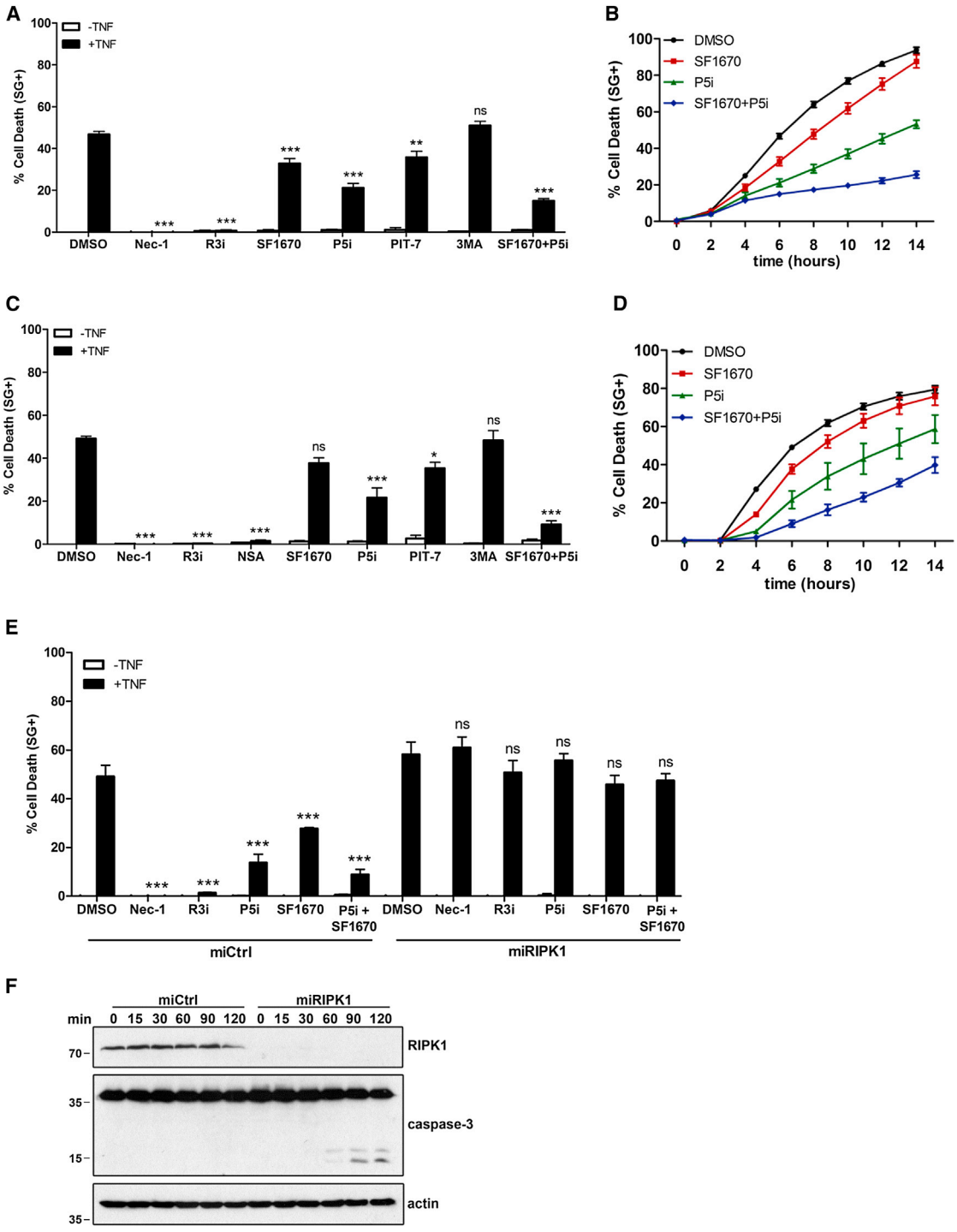

Figure 5. Interfering with the Formation of PI(5)P or PI(4,5)P_2 Inhibits TNF-Induced Necroptosis but Not TNF-Induced Apoptosis

(A–D) L929sAhFas cells (A and B) or FADD$^{-/-}$ Jurkat cells (C and D) were pretreated for 30 min with the indicated compounds and subsequently stimulated by hTNF. Cell death was analyzed over a period of 14 hr by SYTOX Green staining (A and C). Statistical analysis is shown after 6 hr of TNF stimulation (B–D).

(E and F) L929sAhFas cells transduced with either a nontargeting miRNA (miCtrl) or a miRNA targeting RIPK1 (miRIPK1) were pretreated for 30 min with the indicated compounds and subsequently stimulated by hTNF. Cell death was analyzed after 6 hr by SYTOX Green staining (E). These transduced cells were also stimulated with hTNF for the indicated durations and immunoblotted as indicated (F).

Cell death data are presented as mean ± SEM of three independent experiments. Statistical significance was determined by one-way ANOVA followed by a post hoc Bonferroni correction for multiple testing between the control sample (DMSO-treated) and the treated samples. *$p < 0.05$; **$p < 0.01$; ***$p < 0.001$; ns, nonsignificant.

Please cite this article in press as: Dondelinger et al., MLKL Compromises Plasma Membrane Integrity by Binding to Phosphatidylinositol Phosphates, Cell Reports (2014), http://dx.doi.org/10.1016/j.celrep.2014.04.026

minimal essential medium supplemented with 10% FCS and 1× minimal essential medium nonessential amino acid solution (Sigma-Aldrich). FADD$^{-/-}$ Jurkat cells were cultured in RPMI media supplemented with 10% FCS, L-glutamine, sodium pyruvate, and β-mercaptoethanol. For the transfection of HEK293T cells, the cells were seeded at 300,000 per well in a 6-well plate on day 0 and transfected on day 1 with 1 μg DNA using jetPEI transfection reagent (Polyplus-transfection) according to the manufacturer's instructions. Transduction of the L929sAhFas was done by lentiviral transduction. A total of 1 × 10^6 HEK293T cells were transfected using calcium phosphate with either a pLenti6.2-miCtrl or a pLenti6.2-miRIPK1 plasmid in combination with the lentiviral-packaging vectors pMD2-VSVG and pCMV-ΔR8.91. The medium was changed after 6 hr, and this virus-containing supernatant was collected 48 hr posttransfection. The supernatant was then used to infect the L929sAhFas cell line.

Antibodies, Cytokines, and Reagents

The antibodies, cytokines, and reagents used in this manuscript are listed in the Supplemental Experimental Procedures.

Analysis of Cell Death

For HEK293T cells, SYTOX Green (Invitrogen) was added 24 hr after transfection at a final concentration of 5 μM. SYTOX Green intensity was measured by a FLUOstar Omega fluorescence plate reader (BMG Labtech) using an excitation filter of 485 nm, an emission filter of 520 nm, gains set at 1,100, 40 flashes per well, and orbital averaging with a diameter of 7 mm. Afterward, all cells were lysed by adding Triton X-100 at a final concentration of 0.1%, and SYTOX Green intensity was measured again.

L929sAhFas, FADD$^{-/-}$ Jurkat, or HT-29 cells were seeded at 10,000, 50,000, or 40,000 cells per well, respectively, in triplicates in a 96-well plate. The next day, cells were pretreated with the indicated compounds for 30 min and then stimulated with human TNF (hTNF) (600 IU/ml) in the presence of 5 μM SYTOX Green. SYTOX Green intensity was measured at intervals of 1 hr by using a FLUOstar Omega fluorescence plate reader, with an excitation filter of 485 nm, emission filter of 520 nm, gains set at 1,100, 20 flashes per well, and orbital averaging with a diameter of 3 mm.

In both cases, percentage of cell death was calculated as (induced fluorescence − background fluorescence) / (maximal fluorescence − background fluorescence) × 100. The maximal fluorescence is obtained by full permeabilization of the cells by using Triton X-100 at a final concentration of 0.1%. All cell death data are presented as mean ± SEM of three independent experiments.

MLKL Subcellular Localization Using Confocal Microscopy

Two days before imaging, HEK293T cells were seeded at 10,000 cells per well in an 8-well Ibiditreat μ-slide from Ibidi. The next day, cells were transfected with 50 ng of the indicated pLenti6-strep-hMLKL-EGFP mutants using jetPEI transfection reagent according to the company's instructions. After 24 hr, cells were fixed with 4% paraformaldehyde for 15 min at room temperature. Images were acquired using a Leica TCS SP5 confocal system with a 63× HCX PL Apo 1.4 oil-immersion objective, with a format of 1,024 × 1,024, a line average of 4 at 400 Hz, and a zoom of 2.5. Stacks were imaged at a z step of 83.9. The bright-field images were acquired with the 633 laser line, with a gain of 300. The GFP fluorescence was imaged with the 488 argon laser line at 28%, bandwidth of 498–589, with a gain of 893. Deconvolution of the GFP signal was performed on Volocity software (PerkinElmer), and image reconstruction was performed using ImageJ.

Lipid and PIP Arrays

Recombinant GST-human MLKL (hMLKL) 1–210 and GST-hMLKL 1–210 9posE were purified from *E. coli* as explained in the Supplemental Experimental Procedures. PIP and lipid strips were purchased from Echelon Biosciences. Both strips were blocked overnight at 4°C in buffer A (PBS [pH 7.4], 3% [w/v] fatty acid-free BSA). A total of 2.5 μg recombinant protein was incubated on lipid and PIP strips for 1 hr at room temperature in buffer B (PBS [pH 7.4], 0.1% [v/v] Tween 20, 3% [w/v] fatty acid-free BSA). Binding of the proteins to the lipids was revealed with goat anti-GST (GE Healthcare) or rabbit anti-MLKL (Sigma-Aldrich) in buffer B and visualized by infrared fluorescence detection using the Odyssey system (LI-COR Biosciences).

Liposome Assay

Recombinant GST-hMLKL 1–210 and GST-hMLKL 1–210 9posE were purified from *E. coli* as explained in the Supplemental Experimental Procedures. CF-containing liposomes were prepared as described before by Antonsson et al. (1997) but with a modified lipid composition. Briefly, 1 mg lipid containing 95% (mol %) PC and 5% (mol %) PI, PI(5)P, PI(4,5)P_2, or PI(3,4,5)P_3 was dried under nitrogen and solubilized in 1 ml PBS (pH 7.4) containing 20 mM CF (purity >99%) and 30 mg of octyl glucoside/ml. Incubation was carried out for 3 hr at 20°C. Liposomes were then isolated after filtering through a Sephadex G-25 column (1.5 × 20 cm) and dialyzed overnight against PBS at 4°C. Liposomes were diluted to give a suitable fluorescence measurement. Recombinant proteins were added as indicated in the figures, and the change in fluorescence was recorded as a function of time with excitation at 488 nm and emission at 520 nm using a CYT3F Cytation3 Cell Imaging Multi-Mode Microplate Reader (Molecular Devices).

SUPPLEMENTAL INFORMATION

Supplemental Information includes Supplemental Experimental Procedures and four figures and can be found with this article online at http://dx.doi.org/10.1016/j.celrep.2014.04.026.

ACKNOWLEDGMENTS

We thank Amin Bredan for editing the manuscript. We thank Sarah Faherty O'Donnell and Julie De Keyser for technical assistance. P.V. is senior full professor at Ghent University and holder of a Methusalem grant. Y.D. is holder of a PhD fellowship from the Agency for Innovation by Science and Technology (IWT). W.D. has a research professor position at Ghent University. M.J.M.B. has a tenure track position in the Multidisciplinary Research Program of Ghent University (GROUP-ID). P.H. and A.G. are paid by a VIB grant, and R.R., I.B., and K.W. are paid by the Methusalem grant. Research in the P.V. group is supported by Belgian grants (Interuniversity Attraction Poles, IAP 7/32), Flemish grants (Research Foundation Flanders: FWO G.0875.11, FWO G.0973.11, FWO G.0A45.12N, and FWO G.0787.13N; and a Methusalem grant BOF09/01M00709), Ghent University grants (MRP, GROUP-ID consortium), a grant from the Foundation against Cancer (F94), and grants from the VIB. RIP3 inhibitor GSK'840 is available under an MTA agreement, and requests should be addressed to P.J.G. (peter.j.gough@gsk.com). C.A.S., R.W.M., J.B., and P.J.G. are employees of GlaxoSmithKline.

Received: February 10, 2014
Revised: April 9, 2014
Accepted: April 18, 2014
Published: May 8, 2014

REFERENCES

Antonsson, B., Conti, F., Ciavatta, A., Montessuit, S., Lewis, S., Martinou, I., Bernasconi, L., Bernard, A., Mermod, J.J., Mazzei, G., et al. (1997). Inhibition of Bax channel-forming activity by Bcl-2. Science *277*, 370–372.

Biton, S., and Ashkenazi, A. (2011). NEMO and RIP1 control cell fate in response to extensive DNA damage via TNF-α feedforward signaling. Cell *145*, 92–103.

Cai, Z., Jitkaew, S., Zhao, J., Chiang, H.C., Choksi, S., Liu, J., Ward, Y., Wu, L.G., and Liu, Z.G. (2014). Plasma membrane translocation of trimerized MLKL protein is required for TNF-induced necroptosis. Nat. Cell Biol. *16*, 55–65.

Chen, W., Zhou, Z., Li, L., Zhong, C.Q., Zheng, X., Wu, X., Zhang, Y., Ma, H., Huang, D., Li, W., et al. (2013). Diverse sequence determinants control human and mouse receptor interacting protein 3 (RIP3) and mixed lineage kinase domain-like (MLKL) interaction in necroptotic signaling. J. Biol. Chem. *288*, 16247–16261.

Chen, X., Li, W., Ren, J., Huang, D., He, W.T., Song, Y., Yang, C., Li, W., Zheng, X., Chen, P., and Han, J. (2014). Translocation of mixed lineage kinase

domain-like protein to plasma membrane leads to necrotic cell death. Cell Res. *24*, 105–121.

Cho, W., and Stahelin, R.V. (2005). Membrane-protein interactions in cell signaling and membrane trafficking. Annu. Rev. Biophys. Biomol. Struct. *34*, 119–151.

Cho, Y.S., Challa, S., Moquin, D., Genga, R., Ray, T.D., Guildford, M., and Chan, F.K. (2009). Phosphorylation-driven assembly of the RIP1-RIP3 complex regulates programmed necrosis and virus-induced inflammation. Cell *137*, 1112–1123.

Czabotar, P.E., Lessene, G., Strasser, A., and Adams, J.M. (2014). Control of apoptosis by the BCL-2 protein family: implications for physiology and therapy. Nat. Rev. Mol. Cell Biol. *15*, 49–63.

Dondelinger, Y., Aguileta, M.A., Goossens, V., Dubuisson, C., Grootjans, S., Dejardin, E., Vandenabeele, P., and Bertrand, M.J. (2013). RIPK3 contributes to TNFR1-mediated RIPK1 kinase-dependent apoptosis in conditions of cIAP1/2 depletion or TAK1 kinase inhibition. Cell Death Differ. *20*, 1381–1392.

Duprez, L., Takahashi, N., Van Hauwermeiren, F., Vandendriessche, B., Goossens, V., Vanden Berghe, T., Declercq, W., Libert, C., Cauwels, A., and Vandenabeele, P. (2011). RIP kinase-dependent necrosis drives lethal systemic inflammatory response syndrome. Immunity *35*, 908–918.

Garcia, P., Gupta, R., Shah, S., Morris, A.J., Rudge, S.A., Scarlata, S., Petrova, V., McLaughlin, S., and Rebecchi, M.J. (1995). The pleckstrin homology domain of phospholipase C-delta 1 binds with high affinity to phosphatidylinositol 4,5-bisphosphate in bilayer membranes. Biochemistry *34*, 16228–16234.

He, S., Wang, L., Miao, L., Wang, T., Du, F., Zhao, L., and Wang, X. (2009). Receptor interacting protein kinase-3 determines cellular necrotic response to TNF-alpha. Cell *137*, 1100–1111.

Kaczmarek, A., Vandenabeele, P., and Krysko, D.V. (2013). Necroptosis: the release of damage-associated molecular patterns and its physiological relevance. Immunity *38*, 209–223.

Li, J., McQuade, T., Siemer, A.B., Napetschnig, J., Moriwaki, K., Hsiao, Y.S., Damko, E., Moquin, D., Walz, T., McDermott, A., et al. (2012). The RIP1/RIP3 necrosome forms a functional amyloid signaling complex required for programmed necrosis. Cell *150*, 339–350.

Linkermann, A., Bräsen, J.H., Darding, M., Jin, M.K., Sanz, A.B., Heller, J.O., De Zen, F., Weinlich, R., Ortiz, A., Walczak, H., et al. (2013). Two independent pathways of regulated necrosis mediate ischemia-reperfusion injury. Proc. Natl. Acad. Sci. USA *110*, 12024–12029.

Mocarski, E.S., Upton, J.W., and Kaiser, W.J. (2012). Viral infection and the evolution of caspase 8-regulated apoptotic and necrotic death pathways. Nat. Rev. Immunol. *12*, 79–88.

Murphy, J.M., Czabotar, P.E., Hildebrand, J.M., Lucet, I.S., Zhang, J.G., Alvarez-Diaz, S., Lewis, R., Lalaoui, N., Metcalf, D., Webb, A.I., et al. (2013). The pseudokinase MLKL mediates necroptosis via a molecular switch mechanism. Immunity *39*, 443–453.

Parker, M.W., and Feil, S.C. (2005). Pore-forming protein toxins: from structure to function. Prog. Biophys. Mol. Biol. *88*, 91–142.

Rameh, L.E., Arvidsson, Ak., Carraway, K.L., 3rd, Couvillon, A.D., Rathbun, G., Crompton, A., VanRenterghem, B., Czech, M.P., Ravichandran, K.S., Burakoff, S.J., et al. (1997). A comparative analysis of the phosphoinositide binding specificity of pleckstrin homology domains. J. Biol. Chem. *272*, 22059–22066.

Remijsen, Q., Goossens, V., Grootjans, S., Van den Haute, C., Vanlangenakker, N., Dondelinger, Y., Roelandt, R., Bruggeman, I., Goncalves, A., Bertrand, M.J., et al. (2014). Depletion of RIPK3 or MLKL blocks TNF-driven necroptosis and switches towards a delayed RIPK1 kinase-dependent apoptosis. Cell Death Dis. *5*, e1004.

Salim, K., Bottomley, M.J., Querfurth, E., Zvelebil, M.J., Gout, I., Scaife, R., Margolis, R.L., Gigg, R., Smith, C.I., Driscoll, P.C., et al. (1996). Distinct specificity in the recognition of phosphoinositides by the pleckstrin homology domains of dynamin and Bruton's tyrosine kinase. EMBO J. *15*, 6241–6250.

Suh, B.C., and Hille, B. (2008). PIP2 is a necessary cofactor for ion channel function: how and why? Annu Rev Biophys *37*, 175–195.

Sun, L., Wang, H., Wang, Z., He, S., Chen, S., Liao, D., Wang, L., Yan, J., Liu, W., Lei, X., and Wang, X. (2012). Mixed lineage kinase domain-like protein mediates necrosis signaling downstream of RIP3 kinase. Cell *148*, 213–227.

Tait, S.W., Oberst, A., Quarato, G., Milasta, S., Haller, M., Wang, R., Karvela, M., Ichim, G., Yatim, N., Albert, M.L., et al. (2013). Widespread mitochondrial depletion via mitophagy does not compromise necroptosis. Cell Rep *5*, 878–885.

Vanden Berghe, T., Vanlangenakker, N., Parthoens, E., Deckers, W., Devos, M., Festjens, N., Guerin, C.J., Brunk, U.T., Declercq, W., and Vandenabeele, P. (2010). Necroptosis, necrosis and secondary necrosis converge on similar cellular disintegration features. Cell Death Differ. *17*, 922–930.

Vanden Berghe, T., Linkermann, A., Jouan-Lanhouet, S., Walczak, H., and Vandenabeele, P. (2014). Regulated necrosis: the expanding network of non-apoptotic cell death pathways. Nat. Rev. Mol. Cell Biol. *15*, 135–147.

Vanlangenakker, N., Vanden Berghe, T., Krysko, D.V., Festjens, N., and Vandenabeele, P. (2008). Molecular mechanisms and pathophysiology of necrotic cell death. Curr. Mol. Med. *8*, 207–220.

Vanlangenakker, N., Bertrand, M.J., Bogaert, P., Vandenabeele, P., and Vanden Berghe, T. (2011). TNF-induced necroptosis in L929 cells is tightly regulated by multiple TNFR1 complex I and II members. Cell Death Dis. *2*, e230.

Wang, L., Du, F., and Wang, X. (2008). TNF-alpha induces two distinct caspase-8 activation pathways. Cell *133*, 693–703.

Wang, Z., Jiang, H., Chen, S., Du, F., and Wang, X. (2012). The mitochondrial phosphatase PGAM5 functions at the convergence point of multiple necrotic death pathways. Cell *148*, 228–243.

Wang, H., Sun, L., Su, L., Rizo, J., Liu, L., Wang, L.F., Wang, F.S., and Wang, X. (2014). Mixed lineage kinase domain-like protein MLKL causes necrotic membrane disruption upon phosphorylation by RIP3. Mol. Cell *54*, 133–146.

Wu, J., Huang, Z., Ren, J., Zhang, Z., He, P., Li, Y., Ma, J., Chen, W., Zhang, Y., Zhou, X., et al. (2013). Mlkl knockout mice demonstrate the indispensable role of Mlkl in necroptosis. Cell Res. *23*, 994–1006.

Xie, T., Peng, W., Yan, C., Wu, J., Gong, X., and Shi, Y. (2013). Structural insights into RIP3-mediated necroptotic signaling. Cell Rep *5*, 70–78.

Yeung, T., Terebiznik, M., Yu, L., Silvius, J., Abidi, W.M., Philips, M., Levine, T., Kapus, A., and Grinstein, S. (2006). Receptor activation alters inner surface potential during phagocytosis. Science *313*, 347–351.

Zhang, D.W., Shao, J., Lin, J., Zhang, N., Lu, B.J., Lin, S.C., Dong, M.Q., and Han, J. (2009). RIP3, an energy metabolism regulator that switches TNF-induced cell death from apoptosis to necrosis. Science *325*, 332–336.

Zhao, J., Jitkaew, S., Cai, Z., Choksi, S., Li, Q., Luo, J., and Liu, Z.G. (2012). Mixed lineage kinase domain-like is a key receptor interacting protein 3 downstream component of TNF-induced necrosis. Proc. Natl. Acad. Sci. USA *109*, 5322–5327.